

**Strength functions, entropies, and duality in weakly to strongly interacting fermionic systems**

D. Angom, S. Ghosh, and V. K. B. Kota\*

*Physical Research Laboratory, Ahmedabad 380 009, India*

(Received 6 January 2004; published 23 July 2004)

We revisit statistical wave function properties of finite systems of interacting fermions in the light of strength functions and their participation ratio and information entropy. For weakly interacting fermions in a mean-field with random two-body interactions of increasing strength  $\lambda$ , the strength functions  $F_k(E)$  are well known to change, in the regime where level fluctuations follow Wigner's surmise, from Breit-Wigner to Gaussian form. We propose an ansatz for the function describing this transition which we use to investigate the participation ratio  $\xi_2$  and the information entropy  $S^{\text{info}}$  during this crossover, thereby extending the known behavior valid in the Gaussian domain into much of the Breit-Wigner domain. Our method also allows us to derive the scaling law  $\lambda_d \sim 1/\sqrt{m}$  ( $m$  is number of fermions) for the duality point  $\lambda = \lambda_d$ , where  $F_k(E)$ ,  $\xi_2$ , and  $S^{\text{info}}$  in both the weak ( $\lambda=0$ ) and strong mixing ( $\lambda=\infty$ ) basis coincide. As an application, the ansatz function for strength functions is used in describing the Breit-Wigner to Gaussian transition seen in neutral atoms CeI to SmI with valence electrons changing from 4 to 8.

DOI: 10.1103/PhysRevE.70.016209

PACS number(s): 05.45.Mt, 05.30.-d, 32.30.-r, 71.23.An

**I. INTRODUCTION**

There are many physical systems which are statistically well described by the so-called embedded random matrix ensembles of fermions, representing particles subjected to a one-body mean-field potential (defining a set of single-particle levels), and interacting with a random two-body potential. Examples include heavy nuclei [1–5], natural [6,7], or artificial atoms (quantum dots) [8,9], and nanometer-scale metallic grains [10]. Similar situations of randomly interacting spin systems occur in the study of spin-glass systems [11], and in the context of quantum information and quantum computation [12]. In some of these applications the embedded ensembles are directly used while in others (often in nuclei and atoms) the forms given by the ensembles for density of states and other physical quantities are used. The embedded ensembles are defined as ensembles of Hamiltonians  $\{H\} = h(1) + \lambda\{V(2)\}$ , where  $\{\cdot\}$  denotes an ensemble,  $h(1) = \sum_i \epsilon_i n_i$  is a fixed one-body operator (one can also consider an ensemble  $\{h(1)\}$  defined by a probability distribution  $P(\epsilon_i)$  defined by the single-particle energies  $\epsilon_i$  with average spacing  $\Delta$  which sets the energy scale (one can thus set  $\Delta = 1$  without loss of generality), and  $n_i$  is the number operator for the single-particle state  $|i\rangle$ . Similarly  $V(2)$  is the random two-body interaction with its two-particle matrix elements chosen as independent Gaussian variables with zero center and unit variance. Thus, for  $m$  fermions in  $N$  single-particle states,  $\{H\}$  is a one plus two-body random matrix ensemble (called embedded Gaussian orthogonal ensemble of (1+2)-body interactions [EGOE(1+2)]) [1,2] defined by the parameters  $(m, N, \lambda)$ , where  $\lambda$  is the interaction strength. For convenience, we only consider here EGOE(1+2) for spinless fermions, but extensions to particles with intrinsic angular momentum have also been considered [8,10,13]. In such a

case, the size of the Hilbert space is  $d = \binom{N}{m}$  and another important parameter is the connectivity  $K$  giving the number of directly coupled states;  $K = 1 + m(N-m) + m(m-1)(N-m)(N-m-1)/4$ .

Because of its broad relevance to many, *a priori* different, finite quantum systems, EGOE(1+2)'s have been investigated in detail by many research groups in the recent past [1–5,8–10,12–21]. Most investigations used analytical methods extrapolating from the weak and the strong coupling limit, and relied on numerical calculations in the regime of intermediate values of  $\lambda$ . Focusing on the statistical spectral and wave function properties, the dominant features of EGOE(1+2) that emerged from those investigations can be summarized as:

(1) There is a marker  $\lambda_c$ , such that for  $\lambda > \lambda_c$  the many-body level spacing distribution becomes close to that of the Gaussian Orthogonal Ensemble (GOE) of random matrices [22], while for  $\lambda < \lambda_c$  the level fluctuations are close to Poisson. Using the number of directly coupled states  $K$ , it is established that  $\lambda_c \propto 1/m^2 N$  [16,17]; specifically for  $m=6$  and  $N=12$ ,  $\lambda_c \approx 0.06$  [1].

(2) As  $\lambda$  increases from  $\lambda=0$ , the strength functions  $F_k(E)$  (to be defined in Sec. II) undergo a crossover from a delta-peak, first to a Breit-Wigner (BW), then to a Gaussian form. Related to that crossover, there are two markers  $\lambda_F^{(1,2)}$  such that, for  $\lambda_F^{(1)} \leq \lambda \leq \lambda_F^{(2)}$ , the strength functions are well approximated by a BW form [1,3,14,15,18–20]; the BW form emerges above  $\lambda_F^{(1)}$ , which is exponentially smaller in  $m$  and  $N$  than  $\lambda_c$ . In particular, the BW form starts occurring in the region where the spectral fluctuations are still Poissonian (this is not surprising as the BW form follows even for the equidistant spectrum of background states [23]). The  $\lambda > \lambda_F^{(2)}$  region, with GOE spectral and wave function properties, is called Gaussian domain [3]. From now on we put  $\lambda_F = \lambda_F^{(2)}$ ; note that  $\lambda_F \gg \lambda_c$ . Arguments based on BW spreading widths give  $\lambda_F \propto 1/\sqrt{m}$  [15,20]; for the  $m=6$  and  $N=12$  case,  $\lambda_F \approx 0.2$  [3].

(3) In the Gaussian domain, the participation ratio (PR)

\*Author to whom correspondence should be addressed. Fax: 91-79-26301502; Email address: vkbkota@prl.ernet.in

$\xi_2(E)$  and the exponential of the information entropy ( $\exp[S^{\text{info}}(E)]$ ) (both quantities will be defined in Sec. III) take Gaussian forms when plotted as a function of energy  $E$  [3]. The variances of these Gaussian are  $(1+\zeta^2)/(2\zeta^2)$  and  $1/\zeta^2$ , respectively, where  $\zeta^2 = \sigma_h^2(m)/[\sigma_h^2(m) + \lambda^2\sigma_V^2(m)]$ ;  $\sigma_h(m)$  is the spectrum width produced by  $h(1)$  in the total  $m$ -particle space and similarly  $\sigma_V(m)$  is the width produced by  $V(2)$ . Also, in the BW region, the PR is given by the ratio of the spreading width and the spacing between directly [by  $V(2)$ ] connected states and  $S^{\text{info}} \sim \ln(\text{PR})$  [18] (see also Ref. [24]).

(4) There is a third marker  $\lambda_d$  such that at  $\lambda = \lambda_d$  the strength functions, PR and  $S^{\text{info}}$  expressed in either the  $h(1)$  (i.e.,  $\lambda=0$ ) and  $V(2)$  (i.e.,  $\lambda=\infty$ ) basis will coincide. This is accompanied by a duality transformation relating the values of those quantities in the  $h(1)$  basis to those in the  $V(2)$  basis by  $\lambda \rightarrow \lambda_d^2/\lambda$  [20]. In Sec. V the  $(m, N)$  dependence of  $\lambda_d$  will be shown to be  $\lambda_d \sim 1/\sqrt{m}$  (correcting the previously postulated result  $\lambda_d \sim 1/m^{1/4}$  [20]); for  $m=6$  and  $N=12$ , as we shall see ahead,  $\lambda_d \approx 0.3$ .

It is useful to point out that chaos markers, similar to  $\lambda_c$ ,  $\lambda_F$ , and  $\lambda_d$ , which depend on different types of connectivities [see points (1)–(4) above and also Sec. V], are also found in many other models with interactions; see for example Ref. [25]. Another important result for EGOE(1+2) is that the smoothed (ensemble averaged) density of states takes a Gaussian form independent of the value of  $\lambda$  [1,2,4,26]. Our purpose in this paper is to bring completion to the investigations related to the points (1)–(4) above. In particular, we will introduce an interpolating function for strength functions for the BW to Gaussian transition and apply. It should be pointed out that the BW to Gaussian transition was discussed (in the context of giant resonances in nuclei) first by Lewenkopf and Zelevinsky [27], although not for EGOE(1+2) but for a somewhat different random matrix model with interactions. Also it is important to mention that the existence of the BW domain for nuclei, within the nuclear shell model, was discovered for the first time by Frazier *et al.* [28] for the so-called  $(2s1d)$ -shell nuclei. They showed that the Gaussian strength functions with realistic effective interactions change to BW form as the overall strength of the interaction matrix elements is decreased considerably. In Sec. IV of the present paper we will give the first atomic structure example. Now we will give a preview.

In Sec. II we discuss a variant of the well known Student's  $t$ -distribution [29] [hereafter called  $F_{k;\text{BW-G}}(E)$ ], with a parameter  $\alpha$ , and show that it is well suited for describing the BW to Gaussian transition. Numerical calculations allow us to establish a one-to-one correspondence between  $\alpha$  and the interaction strength  $\lambda$ . In Sec. III, the resulting  $F_{k;\text{BW-G}}(E)$  is used to calculate both PR and  $S^{\text{info}}$ , and comparison is made with direct numerical calculations of these quantities as a function of  $\lambda$ , over the full range of variation of  $\lambda$ , thereby extending previous similar investigations which were restricted to either the Gaussian [3] or BW [18,20] domains. Additional structures in the wave functions can be captured by the structural entropy  $S_{\text{str}} \equiv S^{\text{info}} - \ln \xi_2$ , which measures the amount of information contained in the tails of the strength functions. Results of an analysis of  $S_{\text{str}}$  are also

given in Sec. III. In Sec. IV, the  $F_{k;\text{BW-G}}(E)$  is applied in the analysis of the BW to Gaussian transition one observes as we go from neutral CeI atom to SmI atom. In Sec. V, the existence of a duality transformation in EGOE(1+2) (which was established in Ref. [20]) is discussed and it is shown that, using the results for PR and  $S^{\text{info}}$  in the Gaussian domain, the duality point  $\lambda_d \sim 1/\sqrt{m}$ . Conclusions and final comments are given in Sec. VI.

## II. INTERPOLATING FUNCTION FOR BW TO GAUSSIAN TRANSITION IN STRENGTH FUNCTIONS

Given the mean-field  $h(1)$  basis states  $|k\rangle$  and the expansion of the eigenstates  $|E\rangle$  as  $|E\rangle = \sum_k C_k^E |k\rangle$ , the strength functions  $F_k(E)$ , one for each  $|k\rangle$  state, are defined by

$$F_k(E) = \sum_{E'} |C_k^{E'}|^2 \delta(E - E') = \langle |C_k^E|^2 \rangle (d \rho^H(E)). \quad (1)$$

In Eq. (1),  $\langle \dots \rangle$  indicates an ensemble average,  $d = \binom{N}{m}$  is the  $m$ -particle space dimension and  $\rho^H(E)$  is the normalized (and ensemble averaged) density of states. As mentioned in Sec. I,  $\rho^H(E)$  is in general a Gaussian (often the superscript  $H$  is dropped),

$$\rho^H(E) = \frac{1}{\sqrt{2\pi}\sigma_H(m)} \exp - \frac{\hat{E}^2}{2}; \quad \hat{E} = (E - \epsilon_H(m))/\sigma_H(m), \quad (2)$$

where  $\epsilon_H(m) = \langle H \rangle^m$  is the spectrum centroid and similarly  $\sigma_H(m)$  is the spectral width. The BW and Gaussian (denoted by  $\mathcal{G}$ ) forms of  $F_k(E)$  are,

$$\begin{aligned} F_{k;\text{BW}}(E) &= \frac{1}{2\pi} \frac{\Gamma_k}{(E - E_k)^2 + \Gamma_k^2/4}, F_{k;\mathcal{G}}(E) \\ &= \frac{1}{\sqrt{2\pi}\sigma_k} \exp - \frac{(E - E_k)^2}{2\sigma_k^2}, \end{aligned} \quad (3)$$

where  $E_k = \langle k|H|k\rangle$ . With  $p = \int_{-\infty}^{\mathcal{E}^{(k)}} F_k(E) dE$ , the spreading width  $\Gamma_k = \mathcal{E}_{3/4}^{(k)} - \mathcal{E}_{1/4}^{(k)}$ . Similarly the variance of  $F_k$  is  $\sigma_k^2 = \langle k|H^2|k\rangle - (\langle k|H|k\rangle)^2$ . Both the spreading width  $\Gamma_k$  of the BW and  $\sigma_k$  of the Gaussian strength functions are essentially independent of  $k$  provided one considers  $F_k(E)$ 's with  $E_k$  energies not too far away from the center of the density of the  $|k\rangle$  states [1,3,14]. Similarly, the energies  $E$ 's (of  $H$ ) and  $E_k$ 's will have the same centroid. Moreover, just as the state density  $\rho^H(E)$ , the  $E_k$ 's density, denoted by  $\rho^h(E_k)$  with the meaning of the effective one-body  $\mathbf{h}$  explained below, is also a Gaussian. These results are used throughout this paper and without loss of generality the centroids of  $E$ 's and  $E_k$ 's are set equal to zero. As it is discussed in detail in [3],  $\rho^h(E_k)$  is generated by  $\mathbf{h}$  which is  $h(1)$  plus a small additional term arising from  $V(2)$ . Therefore the width of  $\rho^h(E_k)$  is essentially generated by  $h(1)$  and the  $\sigma_k$ 's are generated by  $V(2)$ . Before proceeding further it should be mentioned that the strength functions are basis dependent and one can define strength functions in the  $V(2)$  basis also. We will turn to this

question when discussing the duality transformation in Sec. V.

For the BW to Gaussian transition we make the following ansatz for  $F_k(E)$ :

$$F_{k:\text{BW-G}}(E; \alpha, \beta) dE = \frac{(\alpha\beta)^{\alpha-(1/2)} \Gamma(\alpha)}{\sqrt{\pi} \Gamma\left(\alpha - \frac{1}{2}\right)} \frac{dE}{[(E - E_k)^2 + \alpha\beta]^\alpha},$$

$$\alpha \geq 1. \quad (4)$$

In Eq. (4) the  $\Gamma()$  are  $\Gamma$ -functions. The parameters  $\alpha$  and  $\beta$  in (4) are in general  $k$  dependent and change with  $\lambda$ . The  $F_{k:\text{BW-G}}$  in (4) gives BW for  $\alpha=1$  and Gaussian for  $\alpha \rightarrow \infty$  (this can be easily checked using Stirling's approximation). As required, it is normalized to unity for any positive value of the continuous parameter  $\alpha$ . For  $2\alpha-1$  an integer,  $F_{k:\text{BW-G}}$  gives the so called *Student's t*-distribution [29], which is well known in statistics. In particular, the *Student's* distribution  $f(x)$  with a parameter  $\nu$  given in Table 5.7 of [29] reduces to (4) with the change  $\alpha = (\nu+1)/2$ ,  $\nu$  a positive integer, and  $x \rightarrow \sqrt{2\nu/(\nu+1)}(E - E_k)/\sqrt{\beta}$ . Note that the construction of  $F_{k:\text{BW-G}}$  in Eq. (4) is similar in spirit to the Brody distribution, interpolating between the Poisson and Wigner-Dyson distributions for nearest neighbor spacing distribution (NNSD) [2]. Also, just as some groups use for the NNSD a linear combination of Poisson and Wigner forms multiplied by  $x$  and  $(1-x)$ , respectively, with  $x$  being the mixing parameter, it is possible to use  $\mu F_{k:\text{BW}}(E) + (1-\mu)F_{k:\text{G}}(E)$  for the BW to Gaussian transition with  $\mu$  ( $0 \leq \mu \leq 1$ ) being the mixing parameter. This simple form is not explored in this paper as it is unlikely that a theory for strength functions for EGOE(1+2) will give this form.

In  $F_{k:\text{BW-G}}(E; \alpha, \beta)$ , the parameter  $\alpha$  is sensitive to shape changes, while the parameter  $\beta$  supplies the energy scale over which  $F_{k:\text{BW-G}}(E; \alpha, \beta)$  extends. Since we focus on the shape transformations,  $\alpha$  is the significant parameter. Firstly, it is easy to see that  $F_{k:\text{BW-G}}(E; \alpha, \beta)$  is an even function of  $E - E_k$ , so that all of its finite odd cumulants vanish (strictly speaking, the centroid is  $E_k$  only for  $\alpha > 1$ ; see Ref. [29]). The variance  $\sigma_k^2$  of  $F_{k:\text{BW-G}}$ , defined only for  $\alpha > 3/2$ , is

$$\sigma_k^2 = \left( \frac{\alpha}{2\alpha - 3} \right) \beta \quad (5)$$

and it is useful to recall that  $\sigma_k^2 \approx \lambda^2 \sigma_{V(2)}^2$  independent of  $k$  [3]. For  $\alpha > 3/2$  one can use (5) to fix  $\beta$  while for  $\alpha \leq 3/2$ , it is the spreading width  $\Gamma_k$  (this is well defined for all  $\alpha$  values) that is useful for fixing the  $\beta$  value. There is no simple expression for  $\Gamma_k$  as a function of  $\alpha$  and  $\beta$  but using (4) this can be calculated numerically. Just as Eq. (5), the excess parameter (also known as Kurtosis) of  $F_{k:\text{BW-G}}$  is  $\gamma_2 = 6/(2\alpha - 5)$  for  $\alpha > 5/2$ . However this expression is not useful in practice; finite range of the spectrum causes large deviations for  $\alpha \approx 2-8$ . Therefore it is more useful (in fitting Eq. (4)) to consider  $\gamma_2$  with the spectrum ranging say from  $-a$  to  $+a$ . Then Eq. (4), with proper normalization gives,

$$\gamma_2(a; \alpha, \beta) = \frac{9 {}_2F_1\left(\frac{5}{2}, \alpha; \frac{7}{2}; -\eta^2\right) {}_2F_1\left(\frac{1}{2}, \alpha; \frac{3}{2}; -\eta^2\right)}{5 \left[ {}_2F_1\left(\frac{3}{2}, \alpha; \frac{5}{2}; -\eta^2\right) \right]^2} - 3, \quad (6)$$

where  $\eta^2 = (a^2/\alpha\beta)$ , and  ${}_2F_1$  a hypergeometric function.

In testing Eq. (4) and also in the applications given ahead in Secs. IV and V we consider the average strength function, hereafter called  $F(E)$ , obtained by averaging  $F_k(E)$  over an interval, much smaller than the width of the  $E_k$ 's spectrum, around  $E_k=0$  (i.e., around the  $E_k$ 's centroid). The spreading width of  $F(E)$  is denoted by  $\Gamma$  [this should not be confused with the  $\Gamma$ -functions in Eq. (4)] and the variance of  $F(E)$  by  $\bar{\sigma}^2$ . In Fig. 1(a) the results of EGOE(1+2) for  $F(E)$  are compared, for the  $m=6, N=12$  system, with the best fit  $F_{k:\text{BW-G}}$  [Eq. (4) with  $E_k=0$ ] for various values of  $\lambda$ . In the fits, for the cases with  $\lambda \geq 0.1$  (for these  $\alpha > 1.6$ ), the  $\beta$  values are fixed using Eq. (5) and the  $\bar{\sigma}$  of  $F(E)$ . Similarly, the spreading width  $\Gamma$  ( $\beta \sim \Gamma^2/4$ ) is used for eliminating  $\beta$  for the specific case of  $\lambda=0.06$  (here  $\alpha=1.2$ ). In the fits, also imposed is the condition that the value of  $\gamma_2$  calculated from Eq. (6) over the spectrum range should be close to the numerical EGOE(1+2) values. As it is seen from Fig. 1, the fits are excellent over a wide range of  $\lambda$  values; in the calculations only  $\lambda \geq 0.06$  are considered (for the system considered in Fig. 1,  $\lambda_c \sim 0.06$ ). Variation of the deduced  $\alpha$  values with  $\lambda$  is shown in Fig. 2. The parameter  $\alpha$  rises slowly up to  $\lambda_F$  (note that  $\lambda_F \sim 0.2$  for the EGOE(1+2) system used in Fig. 1 [3]) and then it starts rising sharply with  $\lambda$ . Finally the  $\alpha$  values start saturating after  $\lambda > \lambda_0 = 0.3$  (the saturation is artificial as the determination of  $\alpha$  for  $\lambda \gg \lambda_0$  is difficult and here  $F(E)$  will be very close to Gaussian). The criteria  $\alpha \sim 4$  and  $\gamma_2 \sim 1$  appear to define  $\lambda_F$ . Figure 2 shows that the BW to Gaussian transition is a sharp transition and therefore studies in BW and Gaussian regimes can be carried out independently, to a good approximation, as it is done in many papers before.

Now we will apply  $F_{k:\text{BW-G}}$  to study PR and  $S^{\text{info}}$  in the region intermediate to BW and Gaussian forms.

### III. PARTICIPATION RATIO AND INFORMATION ENTROPY IN THE BW TO GAUSSIAN TRANSITION REGION

Two important measures of the complexity of eigenstates of interacting systems are the participation ratio and information entropy; see the reviews by Izrailev [30] and Zelevinsky *et al.* [31]. As in the previous section, we expand the Hamiltonian eigenstates in the noninteracting mean-field basis as  $|E\rangle = \sum_k C_k^E |k\rangle$ . Then  $\xi_2(E)$  (i.e., PR) and  $S^{\text{info}}(E)$  are,

$$\xi_2(E) = \left\{ \sum_k |C_k^E|^4 \right\}^{-1}, \quad (7a)$$

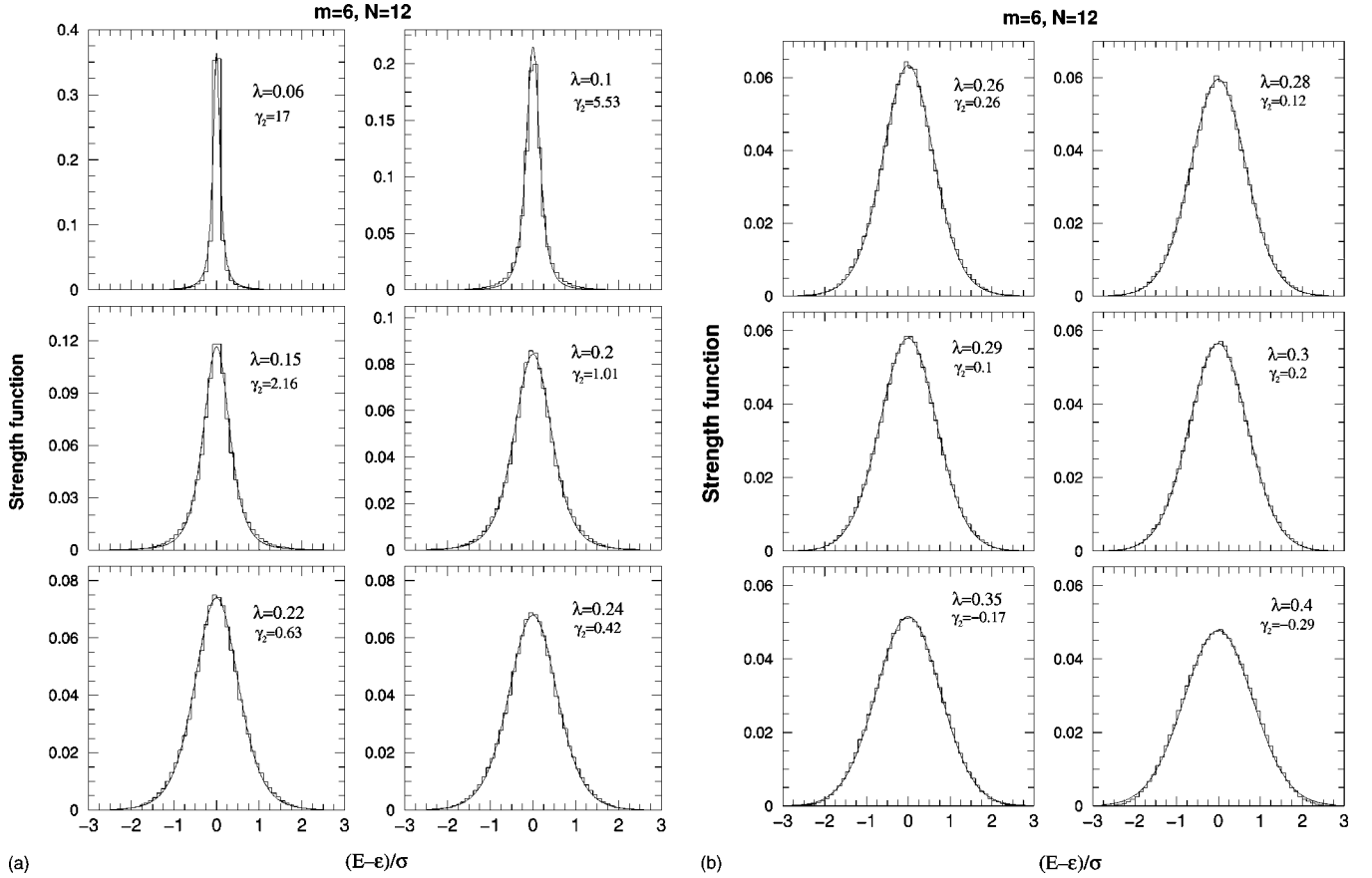


FIG. 1. Strength functions  $F(E)$  for a 20 member EGOE(1+2) for various values of the interaction strength  $\lambda$  in  $\{H\}=h(1)+\lambda\{V(2)\}$  for a system of 6 fermions in 12 single particle states; the matrix dimension is 924. The single particle energies used in the calculations are  $\epsilon_i=(i+1/i), i=1, 2, \dots, 12$  just as in Ref. [1]. In the figures  $F(E)$  is plotted against  $\hat{E}=(E-\epsilon)/\sigma$  where  $\epsilon$  is the spectrum centroid and  $\sigma$  is the width. The histograms are EGOE(1+2) results and the continuous curves are the best fit  $F_{k:BW-G}(E)$  from Eq. (4) with  $E_k=0$ . In constructing the strength functions,  $|C_k^E|^2$  are summed over the basis states  $|k\rangle$  in the energy window  $(\hat{E}_k=0)\pm\hat{\Delta}$  and then the ensemble averaged  $F(\hat{E})$  vs  $\hat{E}$  is constructed as a histogram; the value of  $\hat{\Delta}$  is chosen to be 0.05 for  $\lambda=0.06$  and beyond this  $\hat{\Delta}=0.1$ . Note that  $\hat{E}_k=(E_k-\epsilon)/\sigma$  and, as stated after Eq. (3), here and in all the other calculations,  $\epsilon$  is set equal to zero. Similar results are also obtained for the  $(m=7, N=14)$  system.

$$S^{\text{info}}(E) = - \sum_k |C_k^E|^2 \ln |C_k^E|^2. \quad (7b)$$

The subscript 2 denotes that  $\xi_2$  is the second Rényi entropy [32]. Qualitatively,  $\xi_2$  counts the number of  $\{|k\rangle\}$ -basis states necessary to construct one typical  $|E\rangle$ -state, and is thus often referred to as the Number of Principal Components (NPC) [3,31]. Obviously, both  $\xi_2$  and  $S^{\text{info}}$  are basis dependent, and could as well be defined starting from another expansion. Equation (7) gives their expression with respect to the  $h(1)$  basis and consequently,  $\xi_2$  and  $S^{\text{info}}$  give measures of the spreading of eigenstates over the noninteracting basis as the many-body interaction is made stronger and stronger. In Sec. V, we will deal with these measures defined with respect to the  $V(2)$  basis. As discussed in detail in Ref. [3], for  $\lambda > \lambda_c$ , one can write  $\xi_2$  and  $S^{\text{info}}$  in terms of the strength functions  $F_k(E)$ ,

$$\{\xi_2(E)/\xi_2^{\text{GOE}}\}^{-1} = \frac{1}{[\rho^H(E)]^2} \int_{-\infty}^{\infty} dE_k \rho^h(E_k) [F_k(E)]^2, \quad (8a)$$

$$S^{\text{info}}(E) - S_{\text{GOE}}^{\text{info}} = - \frac{1}{\rho^H(E)} \int_{-\infty}^{\infty} dE_k \rho^h(E_k) F_k(E) \ln \frac{F_k(E)}{\rho^H(E)}. \quad (8b)$$

As it is well known, the GOE values for  $\xi_2$  and  $S^{\text{info}}$  are,

$$\xi_2^{\text{GOE}} = d/3, \quad \exp(S_{\text{GOE}}^{\text{info}}) = 0.48d. \quad (9)$$

Substituting the interpolating  $F_{k:BW-G}(E)$  for  $F_k(E)$  in Eqs. (8a) and (8b), one can study  $\xi_2$  and  $S^{\text{info}}$  as a function of  $\lambda$ . Before going further it is important to consider the correlation coefficient  $\zeta$  that characterizes these measures. For  $\xi_2$  and  $S^{\text{info}}$  in  $h(1)$  ( $\lambda=0$ ) basis,  $\zeta \equiv \zeta_0$ . Given the dimension  $d$ , basis states  $|k\rangle$  and the  $E_k$  energies for a  $m$  particle system,  $(\zeta_0^{(m)})^2$  is defined by (see [3]),

$$(\zeta_0^{(m)})^2 = \frac{\sigma_0^2(m)}{\sigma_H^2(m)},$$

$$\sigma_0^2(m) = d^{-1} \sum_k (E_k - \epsilon_0)^2; \quad \epsilon_0 = d^{-1} \sum_k E_k,$$

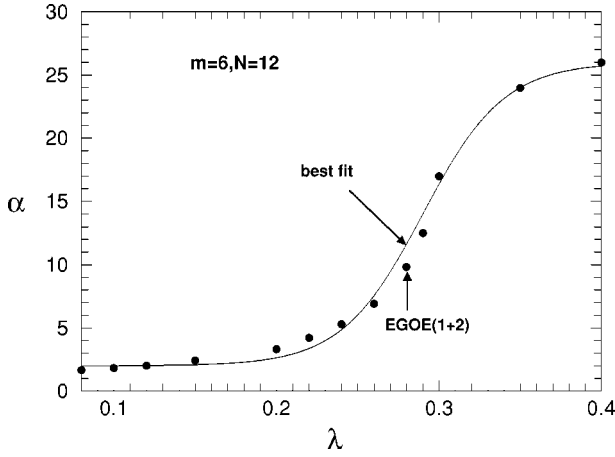


FIG. 2. For  $\lambda \geq 0.08$ ,  $\alpha$  vs  $\lambda$  obtained by fitting the  $F(E)$  in  $h(1)$  basis to the interpolating form  $F_{k:BW-g}$  given by Eq. (4) with  $E_k = 0$ . Results are shown for the EGOE(1+2) system used in Fig. 1. The filled circles give the best fit  $\alpha$  values and the continuous curve, given by  $\alpha = 24/[\exp(-40(\lambda - \lambda_0)) + 1] + 2$  with  $\lambda_0 = 0.29$ , guides the eye. It is curious to note that  $\lambda_0$  is close to  $\lambda_d$ , the duality point discussed in Sec. V. Similar results are also obtained for the ( $m = 7, N = 14$ ) system.

$$\sigma_H^2(m) = d^{-1} \sum_{k \neq k'} |\langle k|H|k' \rangle|^2 + \sigma_0^2(m). \quad (10)$$

In practice, a good approximation to Eq. (10) is

$$(\zeta_0^{(m)})^2 = \frac{\sigma_h^2(m)}{\sigma_h^2(m) + \lambda^2 \sigma_V^2(m)}. \quad (11)$$

Equation (11) is obtained by recognizing that  $\sigma_0^2$  will be very close to  $\sigma_h^2$  and  $\sigma_H^2$  is essentially  $\sigma_h^2 + \lambda^2 \sigma_V^2$  (note that  $\bar{\sigma}^2 = \lambda^2 \sigma_V^2$ ). In fact these results are valid in the dilute limit ( $m \rightarrow \infty, N \rightarrow \infty, m/N \rightarrow 0$ ) and here  $h$  and  $V$  are orthogonal. Even away from the dilute limit they remain to be good approximations (see Fig. 3 ahead for a test). Propagation formulas [1] for  $\sigma_h^2(m)$  and  $\sigma_V^2(m)$  are

$$\sigma_h^2(m) = \frac{m(N-m)}{(N-1)} \sigma_h^2(1) = f^2 \Delta^2, \quad (12a)$$

$$\lambda^2 \sigma_V^2(m) = \frac{m(m-1)(N-m)(N-m-1)N(N-1)}{(N-2)(N-3)} \frac{\lambda^2}{4} = g^2 \lambda^2. \quad (12b)$$

It is possible to write  $\sigma_h^2(1)$ , appearing in (12a), in terms of  $\Delta^2$  and for example for a uniform single particle spectrum,

$$\sigma_h^2(1) = (N+1)(N-1) \frac{\Delta^2}{12}. \quad (13)$$

The  $f$  and  $g$  in (12a) and (12b), respectively, defined by the second equalities in these equations, are used in Sec. V. As shown in Fig. 3, for the  $m=6, N=12$  system, results of the formulas (11) and (12) agree very well with numerical EGOE(1+2) values [obtained via (10)] for  $\zeta_0$ .

Substituting  $F_{k:BW-g}(E)$  for  $F_k(E)$  in Eqs. (8a) and (8b), assuming that the parameters  $\alpha$  and  $\beta$  to be  $k$  independent,

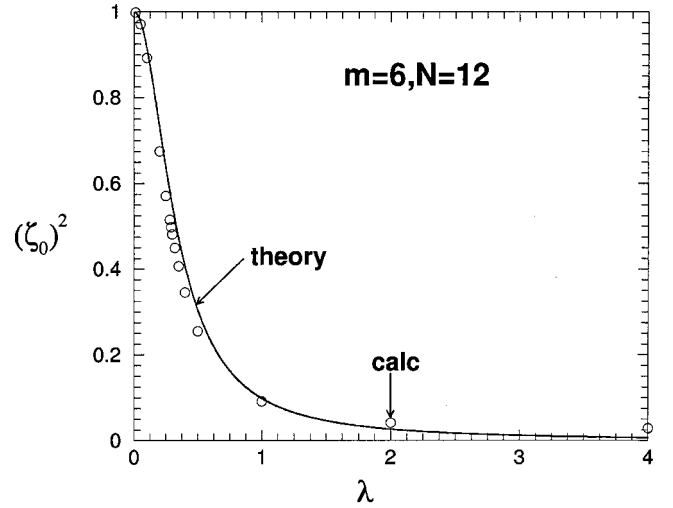


FIG. 3. Square of the correlation coefficient  $\zeta_0$  vs  $\lambda$  for the EGOE(1+2) system used in Fig. 1. Theoretical results (continuous curve) given by Eqs. (11) and (12) are compared with the numerical EGOE(1+2) results (open circles).

using Eq. (5) to eliminate  $\beta$  and simplifying all the variances that enter into Eqs. (8a) and (8b) to  $\zeta^2$  using Eq. (11), it is seen that the integrals in (8a) and (8b) will reduce to integrals with no other parameters except  $\alpha$  and  $\zeta$ . Now the integral in Eq. (8a) for  $\xi_2$  can be further simplified for  $E=0$  [for other  $E$ 's one has to numerically evaluate the integral in Eq. (8a)] and this gives (for  $\alpha > 3/2$ ),

$$\begin{aligned} \xi_2(E=0)/\xi_2^{\text{GOE}} &= \left\{ \sqrt{\frac{2}{(2\alpha-3)}} \frac{\Gamma^2(\alpha)}{\Gamma^2\left(\alpha - \frac{1}{2}\right)} \frac{1}{\sqrt{\zeta^2(1-\zeta^2)}} U\left(\frac{1}{2}, \frac{3}{2}\right) \right. \\ &\quad \left. - 2\alpha, \frac{(2\alpha-3)(1-\zeta^2)}{2\zeta^2} \right\}^{-1}, \end{aligned} \quad (14)$$

where  $U(\dots)$  is hypergeometric-U function [33]. For  $\alpha \leq 3/2$  a compact formula could not be derived but one can use (8a) for numerical evaluations. Similarly, in the case of  $S^{\text{info}}(E=0)$  a simple formula like Eq. (14) could not be obtained for any  $\alpha$  but once again here one can use (8b) for numerical evaluations. In the limit  $\alpha \rightarrow \infty$ , Eqs. (8a) and (8b) can be simplified, for any  $E$ , to give the Gaussian limit formulas derived in [3],

$$\xi_2(E)/\xi_2^{\text{GOE}} = \sqrt{1-\zeta^4} \exp\left(-\frac{\zeta^2 \hat{E}^2}{1+\zeta^2}\right), \quad (15a)$$

$$\exp[S^{\text{info}}(E) - S_{\text{GOE}}^{\text{info}}] = \sqrt{1-\zeta^2} \exp\left(\frac{\zeta^2}{2}\right) \exp\left(-\frac{\zeta^2 \hat{E}^2}{2}\right). \quad (15b)$$

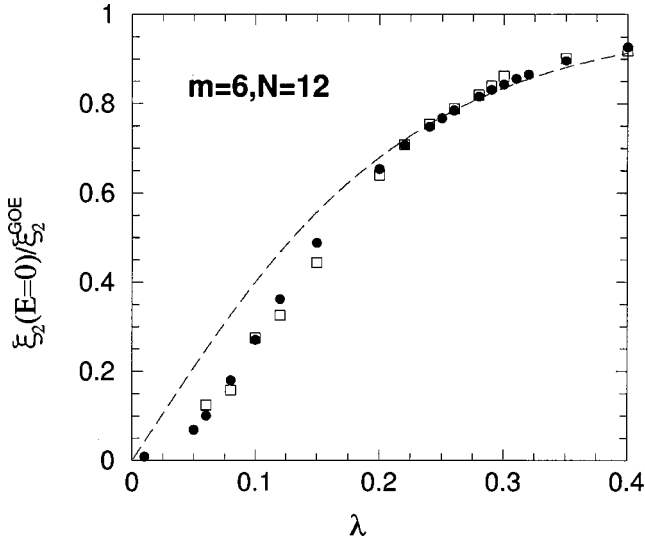


FIG. 4. Participation ratio  $\xi_2(E=0)/\xi_2^{\text{GOE}}$  vs  $\lambda$  for the EGOE(1+2) system used in Fig. 1. Theoretical results given by Eq. (14) (open squares) are compared with the EGOE(1+2) results (filled circles). For comparison, the Gaussian domain result (dashed curve) from Eq. (15a) is also shown.

In Fig. 4, the  $\xi_2(E=0)$  results, from (14) for  $\lambda \geq 0.08$  and from (8a) for  $\lambda = 0.06$ , are compared with numerical EGOE(1+2) calculations for the  $m=6, N=12$  system. The agreement between theory and numerical calculations is good up to  $\lambda \sim 0.06$ . In these calculations the  $\alpha$ -values are read off from Fig. 2 and  $\zeta^2$  from Fig. 3. Comparing with the Gaussian domain results given by (15a), it is seen that they are good for  $\lambda > \lambda_F$  as expected; these results again confirm that  $\lambda_F \sim 0.2$  for the  $m=6, N=12$  system. For  $\lambda < \lambda_F$ , as here the BW structure is more dominant, there will be more localization and hence  $\xi_2$  decreases fast as  $\lambda$  is decreasing and this is seen in Fig. 4. Finally  $\xi_2$  will approach zero for  $\lambda \rightarrow 0$ . The results based on (8a) will not extend to the region  $\lambda \leq \lambda_c$  as here the GOE assumptions used in deriving these equations (see [3]) will fail. Finally, for  $S^{\text{info}}(E=0)$  the results obtained using (8b) are similar to those shown in Fig. 4. This is not surprising as in many numerical calculations (including the present calculations) it is seen that  $S^{\text{info}}(E) \sim \ln(\xi_2(E))$  and therefore only their difference can capture the information not contained in the bulk of  $S^{\text{info}}$  or PR. With this clue, recently it is argued [32] that the structural entropy  $S_{\text{str}}(E) = S^{\text{info}}(E) - \ln[\xi_2(E)]$  is an important measure of complexity [in addition to  $S^{\text{info}}(E)$  or  $\xi_2(E)$ ] in eigenfunctions. More importantly  $S_{\text{str}}$  is free of divergences associated with  $S^{\text{info}}$  and PR. For example,  $\exp(S^{\text{info}})$  and  $\xi_2$  for GOE, as seen from Eq. (9), diverge as the matrix dimension  $d \rightarrow \infty$ . For interacting particle systems it is observed that  $S_{\text{str}}(E=0)$  vs  $\lambda$  (or the disorder in the Anderson model [32]) exhibits a peak. It is then of interest to examine  $S_{\text{str}}$  in terms of the results given in Sec. II.

For small  $\lambda$ , one can estimate  $S_{\text{str}}$  in the BW domain using  $\langle |C_k^E|^2 \rangle = F_{k;\text{BW}}(E) \Delta_m$ , where  $\Delta_m$  gives the many-body level spacing. Inserting this into Eqs. (7a) and (7b) and replacing the sums by integrals over  $E_k$  one gets for  $E=0$ ,

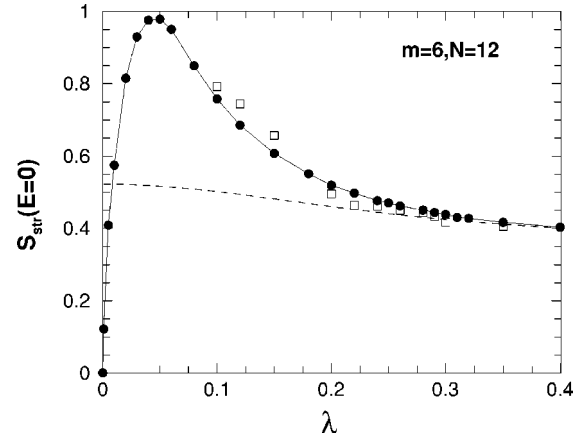


FIG. 5. Structural entropy  $S_{\text{str}}(E=0)$  vs  $\lambda$  for the EGOE(1+2) system used in Fig. 1. Theoretical results calculated using Eqs. (8a), (8b), and (4) (open squares) are compared with the EGOE(1+2) results (filled circles). For comparison, the Gaussian domain result (dashed curve) from (17) is also shown. For guiding the eye, the filled circles are joined by continuous lines. See text for further details.

$$S_{\text{str}}(E=0) = \frac{1}{\pi} \int_{-\tan a}^{\tan a} d\epsilon \frac{\ln(1 + \epsilon^2)}{1 + \epsilon^2} + \ln \left[ \frac{2a + \sin 2a}{2\pi} \right] + \ln \left[ \frac{\pi\Gamma}{2\Delta_m} \right] \left( \frac{2a}{\pi} - 1 \right). \quad (16)$$

In (16),  $a = \arctan(2B/\Gamma)$  where  $2B$  is the  $m$ -particle spectrum span and  $\Gamma \propto \lambda^2$  is the BW spreading width. Equation (16) gives the upper limit for  $S_{\text{str}}(0)$  to be  $\ln 2$  ( $\sim 0.7$ ) and this follows by letting  $B/\Gamma \rightarrow \infty$  (then  $a \rightarrow \pi/2$ ). Similarly in the Gaussian domain, using (15a) and (15b), one has

$$S_{\text{str}}(E=0) = \ln(1.44) + \frac{1}{2} [\zeta^2 - \ln(1 + \zeta^2)]. \quad (17)$$

It should be noted that  $S_{\text{str}}^{\text{GOE}} \approx \ln(1.44)$  independent of  $E$ . An interesting observation (though its significance is not clear) is that for  $\lambda=0$  (then  $\zeta=1$ ) the  $S_{\text{str}}$  is sum of  $S_{\text{str}}^{\text{GOE}}$  and  $S_{\text{str}}$  for a Gaussian function; as shown in [32], for a Gaussian function  $S_{\text{str}} = \frac{1}{2}(1 - \ln 2)$ . Equation (17) shows that, as  $\zeta=0$  for  $\lambda \rightarrow \infty$ ,  $S_{\text{str}}$  approaches the GOE value (0.3689) for very large  $\lambda$ . Except for the formulas (16) and (17), which are derived in the two limiting situations, no analytical results could be derived using the interpolating form (4). However, numerical calculations give some insight. Figure 5 shows EGOE(1+2) results for the  $m=6, N=12$  system for  $S_{\text{str}}(E=0)$  vs  $\lambda$  in the  $h(1)$  basis and their comparison with the results from (8a) and (8b), where  $F_{k;\text{BW}-G}$  given by (4) is used with  $\alpha$  and  $\zeta$  values taken from Figs. 2 and 3, respectively. The  $S_{\text{str}}$  is well described for  $\lambda \geq 0.1$ . Comparing with Eqs. (16) and (17), it is seen that the Gaussian domain formula (17) describes the results for  $\lambda \geq \lambda_F$  while the BW result (16) describes only the trends for  $\lambda$  between 0.1 and  $\lambda_F$  [note that Eq. (16) gives the maximum possible value for  $S_{\text{str}}$  to be 0.7]. More importantly, as seen from Fig. 5 and also from Fig. 4 of [20],  $S_{\text{str}}$  exhibits a peak around a  $\lambda$  value not far from  $\lambda_c$  marker and here the level fluctuations will have a Poisson component.

Thus it is plausible that the peak arises due to large spectral (and strength) fluctuations. A good theory for  $S_{\text{str}}$  generating the observed peak is at present not available.

#### IV. BW TO GAUSSIAN TRANSITION IN NEUTRAL ATOMS CeI TO SmI

Atoms along the lanthanide period are expected to exhibit BW to Gaussian transition in strength functions as the number  $m$  of active valence electrons increases. It is known from the analysis of CeI by Flambaum *et al.* [6] and PrI by Cummings *et al.* [34] that the  $F(E)$  of these atoms with 4 and 5 valence electrons, respectively, are close to BW while those of SmI with 8 valence electrons, as shown in [7], are close to Gaussian. In between are the atoms NdI and PmI with 6 and 7 valence electrons, respectively. It is useful to recall here the relation  $\lambda_F \propto 1/\sqrt{m}$  and this shows that with fixed  $H$ , there will be BW to Gaussian transition as  $m$  is increasing. In order to verify this transition and thus provide a first realistic (atomic structure) application of Eq. (4), we have calculated the strength functions  $F(E)$  for all the five atoms using the same method. Before turning to the results, first the method used in atomic structure calculations is briefly discussed.

The ground state configurations of Ce, Pr, Nd, Pm, and Sm are  $4f5d6s^2(^1G_4)$ ,  $4f^36s^2(^4I_{9/2})$ ,  $4f^46s^2(^5I_4)$ ,  $4f^56s^2(^6H_{5/2})$ , and  $4f^66s^2(^7F_0)$ , respectively. Coupling of the high angular momentum  $5d$  and  $4f$  electrons produce several configurations with strong configuration mixing. Previous work on lanthanide series [35] and Sm I [36] in particular established that an appropriate method to calculate atomic orbitals is the multiconfiguration Dirac-Fock method (MCDF). Details of this method and its implementation are described in [37,38]. In the present study, for a given atom, a series of MCDF calculations are carried out to generate single electron basis set consisting of  $(1-6)s_{1/2}$ ,  $(2-6)p_{1/2}$ ,  $(2-6)p_{3/2}$ ,  $(3-5)d_{3/2}$ ,  $4f_{5/2}$ , and  $4f_{7/2}$  orbitals. Then the basic many-electron wave-functions, called the configuration state functions (CSFs)  $|\gamma_k P J M\rangle$ , where  $P$ ,  $J$ , and  $M$  are parity, total angular momentum, and magnetic quantum numbers respectively and  $\gamma_k$  are the additional quantum numbers needed to define each of the CSFs uniquely, are constructed for a given  $J$  and  $P$ . The CFS's basis in the present calculations consists of single and double excitations from a reference configuration  $4f^l 5d^m 6s^2$  to  $5d$ ,  $6p$ , and  $4f$  shells, where  $l$  and  $m$  are the occupancies of the shells. Finally, the atomic (Dirac-Coulomb) Hamiltonian is diagonalized in the CSF's space of specific  $J$  and  $P$ . This sequence of calculations is repeated for each of the five atoms. Details of  $J^P$ , the reference configuration considered and the number of CSFs generated for each atom are given in Table I. Note that the parity ( $P$ ) is chosen to be same as that of the ground state and  $J$  to be 4 for even and 9/2 for odd cases. For the analysis of strength functions, we choose the CSFs (they are the basis states  $|k\rangle$  in Sec. II) which have close to uniform separation. For example, in Sm only 6500 of the 7325 CSFs generated are considered, the first 200 and last 625 CSFs are excluded. Then, the strength functions  $F(E)$  averaged over 3% of the  $E_k$ 's around their center are constructed for CeI to SmI and compared with Eq. (4).

TABLE I. Details of the angular momentum, the reference configuration considered, and the number of CSFs generated for each of the atoms. The numbers within parentheses are the number of CSFs chosen for the final calculations.

Element	$J^P$	Ref. Config.	Number of CSFs
Ce	$4^-$	$4f5d6s^2$	373 (308)
Pr	$9/2^-$	$4f^36s^2$	1378 (1278)
Nd	$4^+$	$4f^46s^2$	2200 (2000)
Pm	$9/2^-$	$4f^56s^2$	4378 (4178)
Sm	$4^+$	$4f^66s^2$	7325 (6500)

Figure 6 shows that the  $F_{k;\text{BW-G}}(E)$  (Eq. (4) with  $E_k=0$ ) gives excellent description of the calculated  $F(E)$ 's. In applying Eq. (4),  $\beta$  is eliminated using Eq. (5) and then the best fit  $\alpha$  values are deduced. The BW to Gaussian transition is clearly seen in Fig. 6 with  $\alpha$  changing from 1.85 to 14 as we go from CeI to SmI. The calculated  $\gamma_2$  values are also consistent with this transition as they change from 6.44 to 0.46. Comparing with Fig. 1, CeI and PrI atoms are close to  $\lambda \sim 0.1-0.15$  cases [ $F(E)$  is close to BW], NdI and PmI are close to  $\lambda \sim 0.2-0.25$  cases [ $F(E)$  is intermediate to BW and Gaussian] and SmI is close to  $\lambda \sim 0.3$  case [ $F(E)$  is close to Gaussian] of the  $m=6, N=12$  EGOE example. Thus NdI and PmI (calculations for these atoms are reported for the first time in this paper) have  $F(E)$  intermediate to BW and Gaussian forms. For further confirming the BW to Gaussian transition,  $\xi_2(E=0)/\xi_2^{\text{GOE}}$  values are calculated using Eq. (14) and the  $\alpha$  values given in Fig. 6 (used also are the calculated  $\zeta$  values). They change from 0.21 to 0.6 for CeI to SmI and they are close to  $\xi_2(E=0)/\xi_2^{\text{GOE}}$ 's generated by the calculated atomic eigenstates. However there are large fluctuations in  $\xi_2(E)$ , as the atomic calculations produce in general, for many states, more localization than expected from EGOE(1+2); if we average  $\xi_2(E)$  in the neighborhood of  $E=0$ , then the calculated values are  $\sim 20\% - 30\%$  smaller than the values given by Eq. (14). This is already seen in Ce I and PrI in [34] and SmI in [7]. The present calculations confirm this to be a generic behavior. Modifications of EGOE(1+2) for incorporating this property need to be studied but this is for future. Here it suffices to conclude that, from the results in Fig. 6, CeI to SmI exhibit BW to Gaussian transition in  $F(E)$ .

#### V. DUALITY BETWEEN WEAK AND STRONG MIXING LIMITS

For the Hamiltonian  $H=h(1)+\lambda V(2)$  two asymptotic natural basis emerge, the  $\lambda=0$  basis defined by  $h$  and the  $\lambda=\infty$  basis defined by  $V$ . The discussions in Secs. II and III are concerned with strength functions, PR and  $S^{\text{info}}$  in the  $\lambda=0$  basis only. Here we will extend this discussion to the  $\lambda=\infty$  basis and focus on the existence of a duality transformation between the two basis. Recently Jacquod and Varga (JV) [20] showed that a *duality* point  $\lambda_d$  exists where all the statistical wave function properties in these two basis coincide, and that the wave function properties in the noninteracting

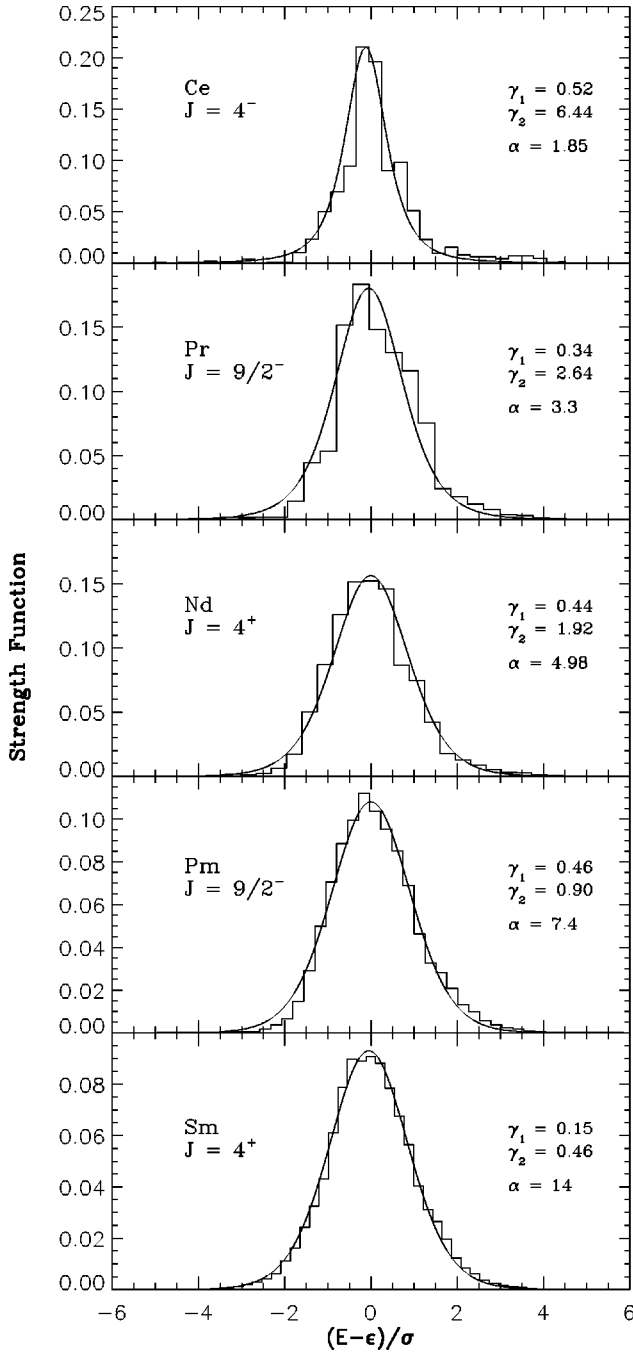


FIG. 6. Strength functions  $F(E)$  for CeI to SmI. Histograms are calculated strength functions and the smooth curves are the best fit  $F_{k;BW-G}(E)$  with  $E_k=0$ . Also given in the figures are the calculated  $\gamma_1$  (skewness) and  $\gamma_2$  (excess) values and the deduced values, of  $\alpha$  characterizing  $F_{k;BW-G}(E)$  with  $E_k=0$ . In the figure,  $\epsilon$  and  $\sigma$  are the spectral centroids and widths. See text for further details.

( $\lambda=0$ ) basis are related to those in the  $\lambda=\infty$  (fully interacting) basis by the duality transformation  $\lambda \leftrightarrow \lambda_d^2/\lambda$ . An ambiguity in JV results lied with the fact that the existence and scaling of the duality point  $\lambda_d$  were derived within the BW approximation for  $F(E)$ , while  $\lambda_d$  explicitly lies outside the BW regime. We therefore extend those theoretical arguments

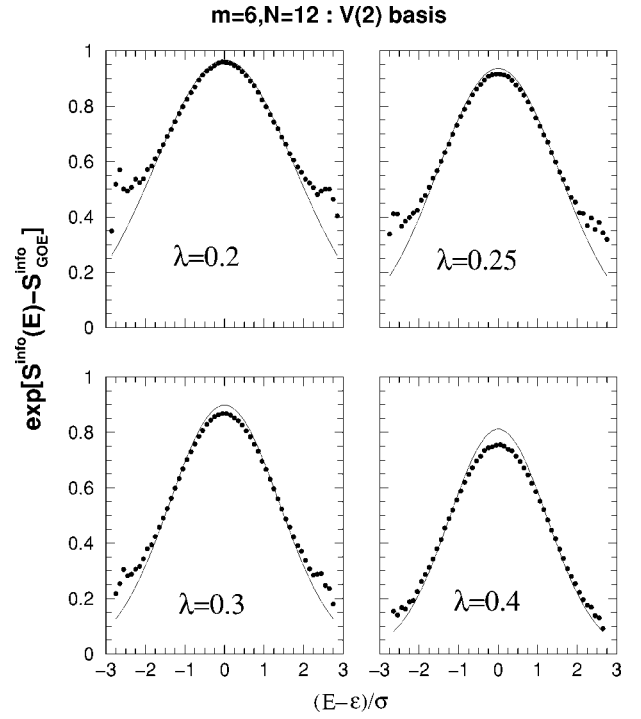


FIG. 7.  $\exp[S^{\text{info}}(E) - S_{\text{GOE}}^{\text{info}}]$  in  $V(2)$  basis (filled circles) for four different  $\lambda$  values for the EGOE(1+2) system used in Fig. 1. The continuous curves are from Eq. (15b) with  $\zeta = \zeta_\infty$ .

by similar ones in the Gaussian approximation, but first let us recall the JV results.

In the noninteracting ( $\lambda=0$ ) basis, the spreading width  $\Gamma^{(0)}$  of  $F(E)$  can be estimated using the Golden Rule. For this, first one has to realize that there are, besides the one-body spacing  $\Delta$ , two important energy scales [16]: the mean spacing between states directly coupled by the two-body interaction  $\Delta_c^{(0)} = B_2^{(0)}/K \approx 4\Delta/Nm^2$  and the average spacing between the  $m$ -particle states  $\Delta_m^{(0)} = B_m^{(0)}/d$ , where  $B_m^{(0)} \approx \sqrt{mN\Delta}$  is the  $m$ -particle spectrum width for  $\lambda \rightarrow 0$  [note that  $B_m^{(0)} \sim \sigma_h(m)$  with  $\sigma_h(m)$  given by (12a) and (13)]. This estimate slightly differs from that of JV where the  $B_m^{(0)}$  was approximated by the  $m$  particle spectrum span. Then, the golden rule gives  $\Gamma^{(0)} \propto \lambda^2/\Delta_c^{(0)} \sim \lambda^2 Nm^2/\Delta$ . With this, in the dilute limit ( $m \ll N$ ), the PR in the  $\lambda=0$  basis is  $\xi_2^{(0)} = \Gamma^{(0)}/\Delta_m^{(0)} \propto \lambda^2 m^{3/2} d/\Delta^2$ . This result differs from the JV estimate given in [20] by the factor  $m^{3/2}$  instead of  $m$ . As is the case for  $\Gamma^{(0)}$ , the Golden Rule also gives a good estimate for the width  $\Gamma^{(\infty)}$  of the  $F(E)$  expressed in the  $\lambda=\infty$  basis. Following JV, it is seen that  $\Gamma^{(\infty)} \sim m(N-m)\Delta^2/\lambda$  and the PR in the  $\lambda=\infty$  basis is  $\xi_2^{(\infty)} = \Gamma^{(\infty)}/\Delta_m^{(\infty)} \propto (\Delta/\lambda)^2 d$ . The duality point is defined by the condition  $\xi_2^{(\infty)}(\lambda_d) = \xi_2^{(0)}(\lambda_d)$  and therefore,

$$\lambda_d \propto \Delta/m^{3/8}. \quad (18)$$

This result [39] is in better agreement with the numerical data presented by JV. They found that  $\lambda_d \sim 1/m^\nu$  with  $\nu \in [0.3, 0.5]$  (one has to keep in mind that most data are not in the dilute limit and that  $\nu$  is extracted from a restricted range of variation of  $m$ ). The previous JV estimate is  $\lambda_d \propto \Delta/m^{1/4}$ .



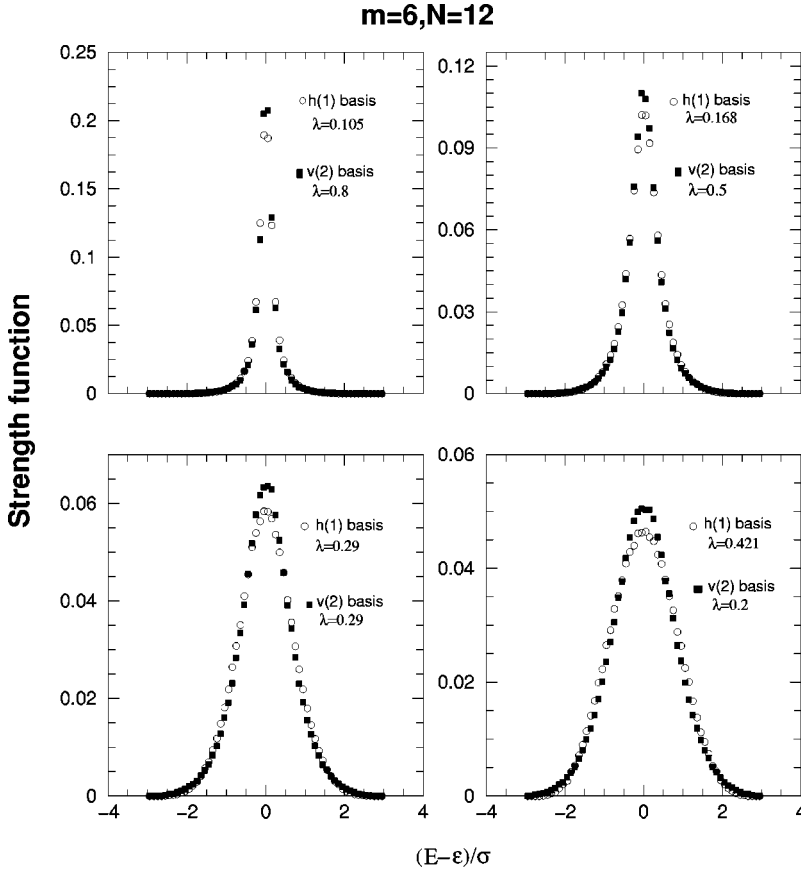


FIG. 8. Strength functions  $F(E)$  in the  $h(1)$  and  $V(2)$  basis for four  $\lambda$  values related by the duality transformation  $\lambda \rightarrow \lambda_d^2/\lambda$ . Results are for the EGOE(1+2) system used in Fig. 1. Here  $\lambda_d = 0.29$ . Similar results for the BW spreading widths are given in Ref. [20] for several EGOE(1+2) systems with  $h(1)$  also chosen to be random.

As stated in the beginning of this section,  $\lambda_d$  lies in the Gaussian domain, i.e.,  $\lambda_d \gg \lambda_F$ . Therefore we will now derive an estimate for  $\lambda_d$  using PR and  $S^{\text{info}}$  in this region. In the Gaussian domain, just as Eqs. (15a) and (15b) describe PR and  $S^{\text{info}}$ , respectively, in the  $h(1)$  basis by substituting  $\zeta_0$  for  $\zeta$  where

$$\zeta_0(\lambda) = \sigma_h / \sqrt{\sigma_h^2 + \lambda^2 \sigma_v^2} = \sqrt{(f^2 \Delta^2) / (f^2 \Delta^2 + g^2 \lambda^2)}, \quad (19)$$

it is expected [by extending in a straight forward manner the arguments in Ref. [3] where  $h(1)$  basis is considered] that in the  $V(2)$  basis also the PR and  $S^{\text{info}}$  will be given by (15a) and (15b) but with  $\zeta = \zeta_\infty$  where,

$$\zeta_\infty(\lambda) = \lambda \sigma_v / \sqrt{\sigma_h^2 + \lambda^2 \sigma_v^2} = \sqrt{(g^2 \lambda^2) / (f^2 \Delta^2 + g^2 \lambda^2)}. \quad (20)$$

The factors  $f^2$  and  $g^2$  in Eqs. (19) and (20) are defined by Eqs. (12) and (13). In Fig. 7 it is verified that Eq. (15b) with  $\zeta = \zeta_\infty$  indeed describes the numerical EGOE(1+2) results for  $S^{\text{info}}(E)$ . Having demonstrated this, it is easily seen that the obvious condition for  $S^{\text{info}}$  and PR [also  $F(E)$ ] to be same in both  $h(1)$  and  $V(2)$  basis is

$$\zeta_0(\lambda_d) = \zeta_\infty(\lambda_d) \Rightarrow \lambda_d = |\Delta f/g|, \quad \zeta^2(\lambda_d) = 0.5. \quad (21)$$

Using Fig. 3 and the condition  $\zeta^2(\lambda_d) = 0.5$  gives for the  $m = 6, N = 12$  example,  $\lambda_d = 0.29$ . In the dilute limit, the  $m$  dependence of  $\lambda_d$  follows from Eqs. (12), (13), and (21),

$$\lambda_d \sim \Delta / (3m)^{1/2}. \quad (22)$$

Thus the Gaussian domain arguments give  $\nu$  (in  $\lambda_d \sim 1/m^\nu$ ) to be 0.5 unlike the improved BW domain arguments which gave 0.375 [see Eq. (18)]. With  $\lambda_d$  defined, a much more significant result that follows from Eqs. (19)–(21) is  $\zeta_\infty(\lambda) = \zeta_0(\lambda_d^2/\lambda)$  and thus there is a duality in EGOE(1+2), i.e., the results in  $h(1)$  and  $V(2)$  basis are related to each other by the duality transformation  $\lambda \rightarrow \lambda_d^2/\lambda$ . As stated before, the same transformation is also derived by JV but using  $\Gamma$  and  $\xi_2$  in the BW domain and this points-out to the general validity of the duality transformation. Strictly speaking  $\lambda_d$  does not lie in the BW domain nor deep into the Gaussian domain. The duality transformation is well tested in Fig. 8 for  $F(E)$  and in Fig. 9 for  $S^{\text{info}}(E)$ . In these calculations  $\lambda_d = 0.29$ . It should be recognized that for the  $F(E)$  in Fig. 8, the variances are  $\zeta_0^2$  and  $\zeta_\infty^2$  in the  $h(1)$  and  $V(2)$  basis, respectively. In the case of  $S^{\text{info}}(E)$  one sees (from Fig. 9) departures, for  $F(E)$  close to Gaussian, in the region well away from the centroid of  $E$  and this could be because the tails of  $F(E)$  display exponential localization [15,28,40]. These disagreements are not seen in [20] as in this work only  $S^{\text{info}}(E=0)$  and  $\xi_2(E=0)$  are studied. It is useful to point-out that there appears to be a close relationship between  $\lambda_d$  and thermodynamics of finite quantum systems. Using the Gaussian domain formulas (see Ref. [21]) for the thermodynamic, information and single particle entropies, it is easily verified that at and around  $\lambda_d$ , all the three entropies will be very close to each other; numerical verification of this result is given in Ref. [21]. Therefore it is

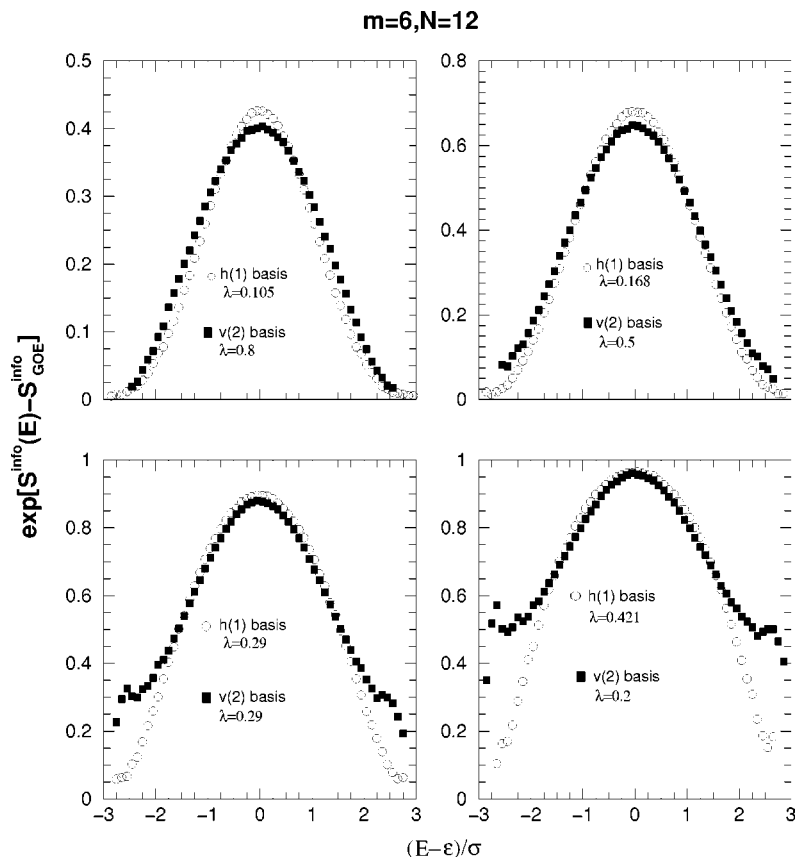


FIG. 9. Same as Fig. 8 but for  $\exp[S_{\text{GOE}}^{\text{info}}(E) - S^{\text{info}}]$ . Similar results for  $\xi_2$  but only at  $E=0$  are given in Ref. [20].

possible to define the region around  $\lambda_d$  as the “thermodynamic region” for interacting particle systems as here different definitions of thermodynamic quantities like entropy will give same results; see Refs. [21,41].

## VI. CONCLUSIONS

In this paper an attempt is made to bring completion to the analytical (in BW and Gaussian domains) and numerical investigations, initiated by a number of research groups, of EGOE(1+2) random matrix model for finite interacting quantum systems. Towards this end, a function describing the BW to Gaussian transition in strength functions is identified [Eq. (4)] and it is used to study participation ratio and information and structural entropy as a function of the interaction strength. Also it is shown, using Gaussian domain results, that the duality point  $\lambda_d$  behaves more like  $\lambda_d$

$\sim 1/\sqrt{m}$  where  $m$  is number of fermions. Applications of these results are given for the BW to Gaussian transition in the series of neutral atoms CeI, PrI, NdI, PmI, and SmI. As for EGOE(1+2), what remains is a rigorous analytical treatment of this random matrix model. This will give for example a theory for  $\alpha$  vs  $\lambda$  (see Fig. 2), a theory for  $S^{\text{info}}$  and PR in the  $\lambda \lesssim \lambda_c$  domain etc. Finally it is important to be reminded that only recently rigorous analytical treatment has started becoming available for the simpler EGOE(2) [26].

## ACKNOWLEDGMENTS

Thanks are due to Ph. Jacquod for a careful reading of the first draft of the paper and for making many suggestions for improving it. The present work was initiated as a result of the correspondence one of the authors (V.K.B.K.) have had with Ph. Jacquod. Thanks are also due to Imre Varga for correspondence in the initial stages of this work.

- 
- [1] V. K. B. Kota, Phys. Rep. **347**, 223 (2001).  
 [2] T. A. Brody, J. Flores, J. B. French, P. A. Mello, A. Pandey, and S. S. M. Wong, Rev. Mod. Phys. **53**, 385 (1981).  
 [3] V. K. B. Kota and R. Sahu, Phys. Rev. E **64**, 016219 (2001).  
 [4] K. K. Mon and J. B. French, Ann. Phys. (N.Y.) **95**, 90 (1975).  
 [5] J. M. G. Gómez, K. Kar, V. K. B. Kota, J. Retamosa, and R. Sahu, Phys. Rev. C **64**, 034305 (2001); V. Velázquez and A. P. Zuker, Phys. Rev. Lett. **88**, 072502 (2002); M. Horoi, J. Kai-

- ser, and V. Zelevinsky, Phys. Rev. C **67**, 054309 (2003); V. K. B. Kota, Ann. Phys. (N.Y.) **306**, 58 (2003).  
 [6] V. V. Flambaum, A. A. Gribakina, G. F. Gribakin, and I. V. Ponomarev, Physica D **131**, 205 (1999); V. V. Flambaum, A. A. Gribakina, G. F. Gribakin, and C. Harabati, Phys. Rev. A **66**, 012713 (2002).  
 [7] Dilip Angom and V. K. B. Kota, Phys. Rev. A **67**, 052508 (2003).

- [8] X. Leyronas, P. G. Silvestrov, and C. W. J. Beenakker, *Phys. Rev. Lett.* **84**, 3414 (2000); Ph. Jacquod and A. D. Stone, *ibid.* **84**, 3938 (2000); *Phys. Rev. B* **64**, 214416 (2001).
- [9] Y. Alhassid, Ph. Jacquod, and A. Wobst, *Phys. Rev. B* **61**, R13357 (2000); *Physica E (Amsterdam)* **9**, 393 (2001); Y. Alhassid and A. Wobst, *Phys. Rev. B* **65**, 041304 (2002).
- [10] T. Papenbrock, L. Kaplan, and G. F. Bertsch, *Phys. Rev. B* **65**, 235120 (2002).
- [11] M. Mézard, G. Parisi, and M. A. Virasoro, *Spin Glass Theory and Beyond* (World Scientific, Singapore, 1987).
- [12] B. Georgeot and D. L. Shepelyansky, *Phys. Rev. E* **62**, 3504 (2000); **62**, 6366 (2000); G. Benenti, G. Casati, and D. L. Shepelyansky, *Eur. Phys. J. D* **17**, 265 (2001); V. V. Flambaum and F. M. Izrailev, *Phys. Rev. E* **64**, 026124 (2001).
- [13] V. K. B. Kota and K. Kar, *Phys. Rev. E* **65**, 026130 (2002).
- [14] V. V. Flambaum, G. F. Gribakin, and F. M. Izrailev, *Phys. Rev. E* **53**, 5729 (1996).
- [15] V. V. Flambaum and F. M. Izrailev, *Phys. Rev. E* **56**, 5144 (1997).
- [16] S. Åberg, *Phys. Rev. Lett.* **64**, 3119 (1990).
- [17] Ph. Jacquod and D. L. Shepelyansky, *Phys. Rev. Lett.* **79**, 1837 (1997).
- [18] B. Georgeot and D. L. Shepelyansky, *Phys. Rev. Lett.* **79**, 4365 (1997).
- [19] V. V. Flambaum and F. M. Izrailev, *Phys. Rev. E* **61**, 2539 (2000); V. K. B. Kota and R. Sahu, e-print nucl-th/0006079.
- [20] Ph. Jacquod and I. Varga, *Phys. Rev. Lett.* **89**, 134101 (2002).
- [21] V. K. B. Kota and R. Sahu, *Phys. Rev. E* **66**, 037103 (2002).
- [22] M. L. Mehta, *Random Matrices*, 2nd ed. (Academic, New York, 1991).
- [23] A. Bohr and B. Mottelson, *Nuclear Structure* (Benjamin, New York, 1969), Vol. 1.
- [24] Ph. Jacquod and D. L. Shepelyansky, *Phys. Rev. Lett.* **75**, 3501 (1995).
- [25] G. P. Berman, F. Borgonovi, F. M. Izrailev, and V. I. Tsifrinovich, *Phys. Rev. E* **65**, 015204(R) (2001).
- [26] L. Benet, T. Rupp, and H. A. Weidenmüller, *Phys. Rev. Lett.* **87**, 010601 (2001); *Ann. Phys. (N.Y.)* **292**, 67 (2001); Z. Pluhar and H. A. Weidenmüller, *ibid.* **297**, 344 (2002).
- [27] C. H. Lewenkopf and V. G. Zelevinsky, *Nucl. Phys.* **569**, 183c (1994).
- [28] N. Frazier, B. A. Brown, and V. Zelevinsky, *Phys. Rev. C* **54**, 1665 (1996).
- [29] A. Stuart and J. K. Ord, *Kendall's Advanced Theory of Statistics*, 5th ed. of Vol. 1: Distribution Theory (Oxford University Press, New York, 1987).
- [30] F. M. Izrailev, *Phys. Rep.* **196**, 299 (1990).
- [31] V. Zelevinsky, B. A. Brown, N. Frazier, and M. Horoi, *Phys. Rep.* **276**, 85 (1996).
- [32] I. Varga and J. Pipek, *Phys. Rev. E* **68**, 026202 (2003).
- [33] *Handbook of Mathematical Functions*, NBS Applied Mathematics Series, edited by M. Abramowitz and I. A. Stegun (U.S. GPO, Washington, D.C., 1964), Vol. 55.
- [34] A. Cummings, G. O'Sullivan, and D. M. Heffernan, *J. Phys. B* **34**, 3407 (2001).
- [35] M. Sekiya, K. Narita, and H. Tatewaki, *Phys. Rev. A* **63**, 012503 (2001).
- [36] Angom Dilip, I. Endo, A. Fukumi, M. Linuma, T. Kondo, and T. Takahasi, *Eur. Phys. J. D* **14**, 271 (2001).
- [37] I. P. Grant and H. M. Quiney, in *Advances in Atomic and Molecular Physics*, edited by D. Bates and B. Bederson (Academic, New York, 1987), Vol 23, p. 37.
- [38] F. Parpia, C. Fischer, and I. Grant, *Comput. Phys. Commun.* **94**, 249 (1996).
- [39] Ph. Jacquod (private communication, 2003).
- [40] W. Wang, F. M. Izrailev, and G. Casati, *Phys. Rev. E* **57**, 323 (1998).
- [41] M. Horoi, V. Zelevinsky, and B. A. Brown, *Phys. Rev. Lett.* **74**, 5194 (1995).